Published OnlineFirst August 25, 2009; DOI: 10.1158/0008-5472.CAN-09-0679

RDEA119/BAY 869766: A Potent, Selective, Allosteric Inhibitor of MEK1/2 for the Treatment of Cancer

Cory Iverson, Gary Larson, Chon Lai, Li-Tain Yeh, Claudia Dadson, Paul Weingarten, Todd Appleby, Todd Vo, Andreas Maderna, Jean-Michel Vernier, Robert Hamatake, Jeffrey N. Miner, and Barry Quart

Research and Development, Ardea Biosciences, Inc., San Diego, California

Abstract

The RAS-RAF-mitogen-activated protein kinase/extracellular signal-regulated kinase (ERK) kinase (MEK)-ERK pathway provides numerous opportunities for targeted oncology therapeutics. In particular, the MEK enzyme is attractive due to high selectivity for its target ERK and the central role that activated ERK plays in driving cell proliferation. The structural, pharmacologic, and pharmacokinetic properties of RDEA119/BAY 869766, an allosteric MEK inhibitor, are presented. RDEA119/BAY 869766 is selectively bound directly to an allosteric pocket in the MEK1/2 enzymes. This compound is highly efficacious at inhibiting cell proliferation in several tumor cell lines *in vitro. In vivo*, RDEA119/BAY 869766 exhibits potent activity in xenograft models of melanoma, colon, and epidermal carcinoma. RDEA119/BAY 869766 exhibits complete suppression of ERK phosphorylation at fully efficacious doses in mice. RDEA119/BAY 869766 shows a tissue selectivity that reduces its potential for central nervous system–related side effects. Using pharmacokinetic and pharmacodynamic data, we show that maintaining adequate MEK inhibition throughout the dosing interval is likely more important than achieving high peak levels because greater efficacy was achieved with more frequent but lower dosing. Based on its longer half-life in humans than in mice, RDEA119/BAY 869766 has the potential for use as a once- or twice-daily oral treatment for cancer. RDEA119/BAY 869766, an exquisitely selective, orally available MEK inhibitor, has been selected for clinical development because of its potency and favorable pharmacokinetic profile. [Cancer Res 2009;69(17):6839–47]

Introduction

Cancer is the second most common cause of death in the United States (one of four deaths; ref. 1). Although progress is being made, as measured by an increase in the 5-year survival rate from ~50% in the 1970s to 66% for people diagnosed with cancer between 1996 and 2002, there is still significant unmet medical need among patients with cancer (1, 2).

The focus of much cancer drug discovery work has shifted toward targeted therapies aimed at genes and pathways that are dysfunctional in human cancer (3). Hyperactivation of cell proliferation, survival, and metastasis pathways can arise from activating gene mutations, gene amplification/overexpression, and/or loss of endogenous tumor suppressors that normally keep these pathways in check (4).

The RAS-RAF-mitogen-activated protein kinase (MAPK)/extracellular signal-regulated kinase (ERK) kinase (MEK)-ERK pathway is constitutively activated in a significant proportion of human tumors often through gain-of-function mutations in *RAS* or *RAF* gene family members or through hyperactivation of upstream receptor tyrosine kinases [e.g., epidermal growth factor (EGF) receptor tyrosine kinase] that transduce signals through this pathway (5). Studies of primary tumor samples and immortalized cancer cell lines have shown constitutive activation of the RAS-RAF-MEK-ERK pathway in several human tumors, including lung, colon, melanoma, thyroid, and pancreatic cancer (6). *BRAF* activating gene mutations are prevalent in melanoma at 66% and thyroid cancer (44% and 24% for papillary and anaplastic thyroid cancer, respectively; refs. 7–9).

Within this pathway lies MEK for which there are two highly homologous genes expressed in humans (*MEK1* and *MEK2*; ref. 10). MEK is downstream of BRAF in the RAS-RAF-MEK-ERK pathway and is critical for transducing signals to ERK (11). *BRAF* activating gene mutations have been shown to predict sensitivity to MEK inhibition across a panel of cancer cell lines (12). This dependency, coupled with a unique hydrophobic pocket within the MEK enzyme that allows for the interaction of highly selective "allosteric" inhibitors, has made MEK an attractive cancer target (13). We describe the structure and activity of RDEA119/BAY 869766 (referred to in this manuscript as RDEA119), an orally available, potent, non–ATP-competitive, highly selective inhibitor of MEK1/2, which is active in human tumor xenograft models and is well tolerated within the therapeutic exposure range in animals.

Materials and Methods

The chemical name of RDEA119 is (*R*)-*N*-(3,4-difluoro-2-(2-fluoro-4-iodophenylamino)-6-methoxyphenyl)-1-(2,3-dihydroxypropyl)cyclopropane-1-sulfonamide, which was synthesized at Ardea Biosciences (Fig. 1*A*). PD0325901 (0494611 L0002): (*S*)-*N*-(2,3-dihydroxy-propoxy)-3,4-difluoro-2-(2-fluoro-4-iodo-phenylamino)-benzamide can be obtained from Selleck Chemicals Co. Ltd.

Preparation and purification of MEK1 for structural studies. A MEK1 cDNA expression construct coding for an NH_2-terminal truncation, MEK1Δ61 (residues 62–393 wild-type truncated form), was cloned into a bacterial expression vector as pET24b-MEK1Δ61 using *Nde*I/*Xho*I sites (10). The COOH-terminal His_6-tag construct was grown at 37°C to an A_{600} of 1.0 and then lowered to 16°C and induced with 3.25 mmol/L isopropyl-L-thio-B-D-galactopyranoside, grown 20 to 24 h as described (10).

Note: Supplementary data for this article are available at Cancer Research Online (http://cancerres.aacrjournals.org/).

Current address for A. Maderna: Wyeth Research, Chemical Sciences, 401 North Middletown Road, Pearl River, NY 10965. Current address for R. Hamatake: Glaxo SmithKline, 5 Moore Drive, Research Triangle Park, NC 27709. Current address for T. Appleby: Gilead Sciences, 333 Lakeside Drive, Foster City, CA 94404. Current address for P. Weingarten: Abraxis Research, 4503 Glencoe Avenue, Marina del Rey, CA 90292.

RDEA119/BAY 869766 has been licensed to Bayer.

Requests for reprints: Jeffrey N. Miner, Ardea Biosciences, Inc., 4939 Directors Place, San Diego, CA 92121. Phone: 858-652-6591; Fax: 858-652-0760; E-mail: jminer@ardeabio.com.

doi:10.1158/0008-5472.CAN-09-0679

Published OnlineFirst August 25, 2009; DOI: 10.1158/0008-5472.CAN-09-0679

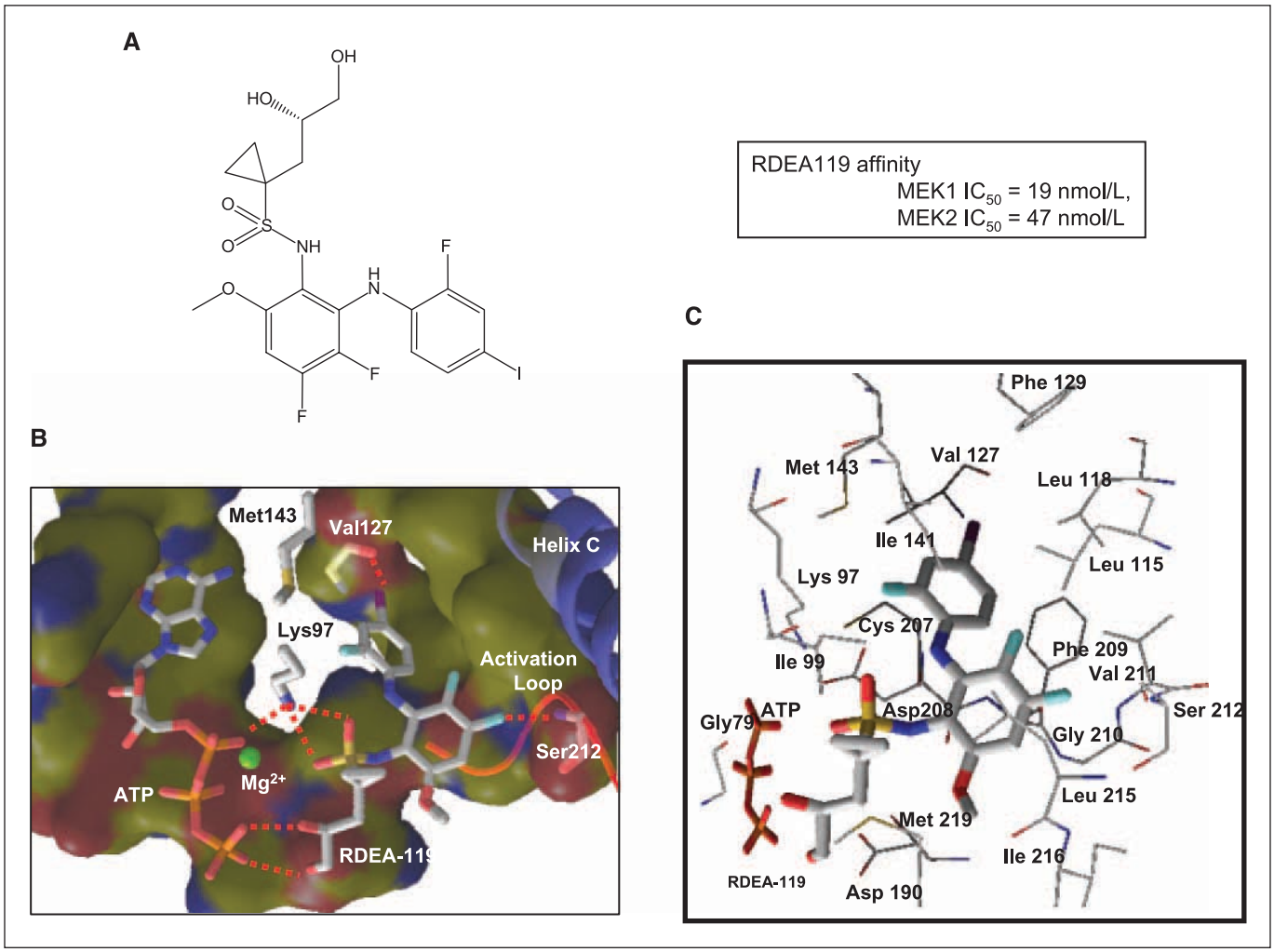

Figure 1. *A,* RDEA119 [(*S*)-*N*-(3,4-difluoro-2-(2-fluoro-4-iodophenylamino)-6-methoxyphenyl)-1-(2,3-dihydroxypropyl)cyclopropane-1-sulfonamide]. The IC_{50}s for interaction with MEK1/2 are shown at right. *B,* view of the ternary complex of human MEK1 bound to Mg-ATP and RDEA119 (PDB: 3E8N) in the active site viewing down through the NH_2 terminus. ATP, RDEA119, and representative residues of protein (i.e., Lys^{97}, Met^{143}, and Ser^{212}) are represented by sticks. Atoms are colored according to type: carbon in gray, oxygen in red, nitrogen in blue, sulfur in yellow, fluorine in light blue, and iodine in purple. *Red dashed lines,* hydrogen bonds or electrostatic interactions. *C,* detailed view of the MEK1 cocrystallized with RDEA119, which binds to an allosteric site adjacent to the Mg-ATP binding region. RDEA119 is represented by large sticks, whereas the MEK1 residues are represented by thin lines and color coded in the same manner as *A*.

Protein-ligand ternary complex formation and cocrystallization. RDEA119 (0.8 μL; 500 mmol/L in 100% DMSO) was added to 0.5 mL of MEK1Δ61 (3 mg/mL) and incubated overnight at 4°C, then brought to 5 mmol/L Mg-ATP and incubated 5 h at 4°C, concentrated, and mixed 1:1 with crystallization reservoir solution [250 mmol/L $NH_4H_2PO_4$, 6% (w/v) PEG 8000, 100 mmol/L malate, 10 mmol/L imidazole], and the drop was allowed to equilibrate over 1 mL of reservoir solution using the hanging drop vapor diffusion technique at 13°C. Frozen MEK1Δ61/RDEA119 cocrystals have unit cell dimensions of a = 82.3 Å, b = 82.3 Å, c = 129.8 Å, $\alpha = 90°$, $\beta = 90°$, and $\gamma = 120°$ and belong to the hexagonal space group $P6_2$.

Data collection and structure determination. A frozen MEK1Δ61/RDEA119 crystal was mounted on an X-ray diffraction system consisting of a RUH3R X-ray generator and a RAXIS IV++ image plate area detector (Rigaku/MSC). A data set of 2.5 Å resolution was collected using 0.5° oscillations and a total ϕ-rotation of 65° and processed, scaled, and reduced (14). The three-dimensional coordinates of only the MEK1 protein atoms from Protein Data Bank entry, 1S9J, were used as the phasing model using the program CNX (15). The initial model was refined against the data initially by treating the MEK1 peptide as a rigid body. Additional rounds of torsion angle annealing and manual adjustment to the model revealed strong difference density for one molecule of ATP, one magnesium ion, and RDEA119. Ligand atoms were added to the model accordingly and included in further rounds of refinement. The final R factor is 21.9% for the model, which includes MEK1 residues (62–222, 224–275, and 306–382), one molecule of ATP, one magnesium ion, 65 water molecules, and the inhibitor RDEA119. Coordinates and structural factors have been deposited into protein data bank,[1] with PDB code 3E8N.

Biochemical kinase assays. The human MEK1 enzyme was purchased from Invitrogen. The active human MEK2 and truncated RAF1 enzyme were purchased from Millipore. Kinase inactive murine ERK2 (mERK2) K52A/T183A was affinity purified from *Escherichia coli* expressed using the pET21a vector. MEK1 kinase activity was determined using mERK2 K52A T183A as the substrate. Recombinant MEK1 enzyme (5 nmol/L) was first activated by 0.02 unit or 1.5 nmol/L of RAF1 in the presence of 25 mmol/L HEPES (pH 7.8), 1 mmol/L $MgCl_2$, 50 mmol/L NaCl, 0.2 mmol/L EDTA, and 50 μmol/L ATP for 30 min at 25°C. The reactions were initiated by adding 2 μmol/L of mERK2 K52A T183A and 2.5 μCi [γ-^{33}P]ATP in a total volume of 20 μL. The MEK2 kinase activity was determined similarly except that activation by RAF1 was not needed and 11 nmol/L of MEK2 enzyme (active) were used in the assays.

[1] http://www.rcsb.org

Published OnlineFirst August 25, 2009; DOI: 10.1158/0008-5472.CAN-09-0679

Kinase profiling was performed by Invitrogen using their SelectScreen Kinase Profiling Service. The Z'-LYTE biochemical assay was used. RDEA119 was assayed in quadruplicate at 10 μmol/L against 205 kinases.

Tumor cell lines and media. A375, SK-Mel-28, A431, Colo205, HT-29, MDA-MB-231, and BxPC3 cell lines were obtained from the American Type Culture Collection. A375, A431, MDA-MB-231, and SK-Mel-28 cells were grown in high-glucose DMEM supplemented with 10% fetal bovine serum (FBS), 1 mmol/L sodium pyruvate, 0.1 mmol/L nonessential amino acids, 2 mmol/L L-glutamine, 100 units/mL penicillin, and 0.1 mg/mL streptomycin. HT-29 cells were grown in McCoy's 5A medium supplemented with 10% FBS, 2 mmol/L L-glutamine, 100 units/mL penicillin, and 0.1 mg/mL streptomycin. BxPC3 cells were grown in RPMI 1640 supplemented with 10% FBS, 1 mmol/L sodium pyruvate, 10 mmol/L HEPES, 2 mmol/L L-glutamine, 100 units/mL penicillin, and 0.1 mg/mL streptomycin. Cells were maintained at 37°C, 5% CO_2, and 100% humidity.

Cellular MEK inhibition. A375, A431, SK-Mel-28, Colo205, HT-29, and BxPC3 cells were plated onto 96-well tissue culture plates (Corning) at densities of 2×10^4, 1.5×10^4, 0.75×10^4, 2×10^4, 4×10^4, and 2×10^4 per well, respectively, with their appropriate growth medium. Plates were incubated overnight to allow cells to adhere. The diluted compounds were added to PBS-washed cells, incubated at 37°C for 20 min in 1% FBS, washed with PBS, and stored at −70°C until further processing.

MEK activity was assayed by measuring the phosphorylation of ERK1 and ERK2 using a phospho-ERK1/2 ELISA kit (BioSource). The mean absorbance measured at 450 nm was converted to percent activity, and average percent activity values were determined from duplicate wells.

Cell growth inhibition assays. For anchorage-dependent growth inhibition experiments, cells were plated in white 384-well plates at 1,000/20 μL/well or white 96-well microplates at 4,000/100 μL/well. After 24-h incubation at 37°C, 5% CO_2, and 100% humidity, compound was incubated for 48 h at 37°C and assayed using CellTiter-Glo. For the 96-well anchorage-independent growth assay, wells of an "ultralow binding" plate (Corning) were filled with 60 μL of a 0.15% agarose solution in complete RPMI 1640. Then, 60 μL of complete RPMI 1640 containing 9,000 cells in 0.15% agarose were added per well. After 24 h, 60 μL of a 3× drug solution in agarose-free complete RPMI 1640 were added. After 7 d, 36 μL of 6× 3-(4,5-dimethylthiazol-2-yl)-5-(3-carboxymethoxyphenyl)-2-(4-sulfophenyl)-2*H*-tetrazolium, inner salt reagent (CellTiter 96 Aqueous, Promega) were added per well. After 2 h at 37°C, absorbance at 490 nm was determined on the M5 plate reader (Molecular Devices). Nonlinear curve fitting was performed using GraphPad Prism 4.

Human tumor xenograft studies. Female athymic nude mice (*nu/nu*, Harlan) were used for all the efficacy studies except for the Colo205 study 2, which used male mice. Studies were performed at Piedmont Research Center in compliance with Association for Assessment and Accreditation of Laboratory Animal Care standards and approved by the review board at Piedmont Research Center. Mice were injected s.c. in the flank with 1×10^6 tumor cells (Colo205 and A431) or ~1 mm^3 tumor fragments (A375 and HT-29). Tumor volumes were monitored by caliper measurements using the formula tumor volume (mm^3) = $(w^2 \times l)/2$, where w = width and l = length in mm of the tumor. For efficacy analysis, treatment was initiated when tumors were 80 to 185 mm^3. RDEA119 was administered by oral gavage once daily or twice daily for 14 d or once every 2 d for 14 doses.

Pharmacodynamic/pharmacokinetic studies. Mice bearing tumors (250–350 mm^3) were dosed by oral gavage with RDEA119 at 2.5, 5, 10, or 25 mg/kg, PD325901 at 10 mg/kg, or vehicle. Three mice from each group were sacrificed at 2, 6, 12, and 24 h after dosing, and plasma, brain, lung, and tumor samples were collected and frozen. Tissue samples were thawed on ice and homogenized in Cell Extraction Buffer (BioSource) at a 10% (v/w) ratio for tumor and 20% (v/w) ratio for brain and lung. Homogenates were incubated on ice for 1 h and centrifuged at 500 × *g* for 5 min. Lysates were transferred to microcentrifuge tubes and further clarified by centrifugation at 14,000 × *g* for 5 min. Lysates were subjected to Western blot analysis probed with a mixture of phospho-p44/42 MAPK antibody and p44/42 MAPK antibody (Cell Signaling). Rat pharmacokinetic/pharmacodynamic studies were conducted as follows: animals from each treatment group were sacrificed at 48 h after dose. Blood samples (~1 mL) were collected for plasma bioanalysis of RDEA119 and PD325901 concentrations by centrifugation at 2,000 rpm for 10 min. Plasma supernatants were aspirated and placed in labeled tubes and stored at −20°C until analysis. Brain and lung samples were also collected (whole organ), weighed, and flash frozen in liquid nitrogen for analysis of total ERK and pERK levels.

Plasma samples were analyzed for RDEA119 using a liquid chromatography-tandem mass spectrometry (LC-MS/MS) method. The method involved the addition of the internal standard ([$^{13}C_6$]RDEA119), protein precipitation with acetonitrile, and final analysis by high-performance LC-MS/MS. An API 5000 triple quadrupole mass spectrometer was used to monitor the precursor→product ion transitions of *m/z* 573→394 and *m/z* 579→400 for RDEA119 and [$^{13}C_6$]RDEA119 in positive electrospray ion mode. The calibration curves covered the concentration range from 10 to 10,000 ng/mL.

Results

RDEA119 is an orally bioavailable small molecule with a molecular weight of 572 g/mol. We conducted a variety of preclinical *in vitro* and *in vivo* studies to determine (*a*) potency against its molecular target MEK, (*b*) selectivity relative to other kinases, (*c*) antiproliferative activity in cell culture systems using both cancer and normal cells, (*d*) *in vivo* antitumor efficacy, (*e*) pharmacokinetic relationships between antitumor efficacy and brain retention, and (*f*) downstream consequences of MEK inhibition on proliferation and/or apoptosis.

Interaction between RDEA119 and the MEK enzyme: X-ray cocrystal structure. RDEA119 potently inhibited MEK activity in enzyme inhibition assays in a non–ATP-competitive manner (MEK1 IC_{50} = 19 nmol/L, MEK2 IC_{50} = 47 nmol/L) determined through incorporation of radioactive phosphate from ATP into ERK as substrate.

To determine the mechanism of inhibition of RDEA119, we cocrystallized RDEA119 with a truncated version of MEK1 that was amenable to crystallization (10). The RDEA119-MEK complex structure reveals that RDEA119 binds to an allosteric site adjacent to the Mg-ATP binding region and interacts extensively with ATP, the activation loop, and other surrounding protein residues through hydrogen bonding and hydrophobic interactions (Fig. 1*B* and *C*). This interaction site is similar to the one identified for the MEK inhibitor PD-318088 (PDB ID: 1S9J; ref. 10). Notably, the sulfonamide moiety hydrogen bonds with the basic side chain of the Lys^{97}, a conserved residue believed to be important for the catalytic activity of protein kinases. The iodine is in electrostatic interaction with backbone C = O of Val^{127}, whereas one of the two fluorines is involved in hydrogen bonding with −NH of Ser^{212}. This inhibitor also forms several contacts to Asp^{208}, Phe^{209}, and Gly^{210}, also known as the DFG motif that is shared across several families of protein kinases. The diol extension of RDEA119 interacts heavily with oxygen atoms of the α and γ phosphate groups of the ATP cofactor, whereas the cyclopropyl of RDEA119 forms contacts with the side chain of Met^{219}. RDEA119 is also engaged in hydrophobic contacts with side chains of residues Ile^{99}, Leu^{115}, Leu^{118}, Phe^{129}, Ile^{141}, Met^{143}, Asp^{190}, Cys^{207}, Asp^{208}, Phe^{209}, Gly^{210}, Val^{211}, Ser^{212}, Leu^{215}, and Ile^{216}. In addition, unlike PD0325901, RDEA119 has a unique cyclopropyl group that is in direct hydrophobic contacts with the side chain of Met^{219} in the A-loop, further stabilizing it in the closed "active" conformation of the enzyme. Such a binding mode thus suggests a noncompetitive mechanism of inhibition of RDEA119 against MEK1, which allows ATP binding but

Published OnlineFirst August 25, 2009; DOI: 10.1158/0008-5472.CAN-09-0679

precludes binding to the substrate ERK, thus preventing ERK phosphorylation (10).

RDEA119 significantly inhibits only MEK1/2 relative to 205 other kinases in a multikinase screen (data not shown). MEK1 and MEK2 were inhibited 97% and 99%, respectively, when tested at 10 μmol/L. Four other kinases (BRAF, BRAF V599E, COT, and RAF1) showed inhibition of >90%; however, these used MEK1 in a cascade assay format and the inhibition in these assays is due to MEK1 inhibition rather than direct inhibition of the other kinases by RDEA119. The kinase-specific assay conditions use a cascade format that has RAF1/MEK/ERK all together in the assay, which phosphorylate an ERK substrate. Therefore, a MEK inhibitor will be flagged as a RAF1 inhibitor in this assay due to reduction of the ERK-specific peptide.

Cellular MEK potency. RDEA119 potently inhibited MEK activity as measured by phosphorylation of ERK1/2 across several human cancer cell lines of different tissue origins and BRAF mutational status with EC_{50} values ranging from 2.5 to 15.8 nmol/L (Table 1A). RDEA119 was significantly bound by human serum albumin (hSA) in these assays as shown by 10- to 30-fold loss of potency in the presence of 1% FBS + 45 mg/mL hSA compared with 1% FBS alone (Table 1A). hSA (45 mg/mL) is the midpoint of the normal serum albumin range in human serum (35–55 mg/mL). Mouse and human plasma protein binding of RDEA119 is 99.6% and 99.8%, respectively (data not shown). These results speak to the availability of the compound in plasma and may affect the activity of a compound *in vivo*; thus, potency in a high protein environment is reduced, but this effect is likely small in humans. The species binding data points towards a smaller free fraction of compound in mouse models, which in turn may underestimate the potency of RDEA119 in man.

Growth inhibition potency and effect of BRAF status. RDEA119 inhibited anchorage-dependent growth of human cancer cell lines harboring the gain-of-function V600E BRAF mutant with GI_{50} values ranging from 67 to 89 nmol/L (Table 1A). In contrast, RDEA119 had significantly less growth-inhibitory potency against cell lines with wild-type BRAF (A431 cells) or MDA-MB-231 cells harboring a BRAF mutation G464V that shows minimal (<2-fold increase) enhancement of inherent kinase activity (Table 1A; ref. 16). Interestingly, under anchorage-independent conditions, GI_{50} values for all cell lines tested were similar (40–84 nmol/L; Table 1A). MDA-MB-231 and A431 cells were significantly more sensitive to RDEA119 under anchorage-independent conditions, suggesting increased dependence on the MEK pathway. These concentrations of RDEA119 had minimal or no effect on the growth of primary human hepatocytes or human renal proximal tubule epithelial cells (data not shown). Inhibition of A375 cell proliferation by RDEA119 was primarily accounted for by cell cycle arrest rather than apoptosis for two reasons: (*a*) cellular membrane integrity (assessed by adenylate kinase release) was minimally affected by drug treatment (data not shown) and (*b*) flow cytometry revealed a G_1-phase cell cycle arrest with little if any sub-G_1 population (Supplementary Data).

Antitumor efficacy of RDEA119 in multiple human tumor xenograft models. The human melanoma A375 tumor xenograft was found to be sensitive to RDEA119 treatment (Table 1B; Fig. 2*A*) with 54% and 68% tumor growth inhibition (TGI) seen with 25 and 50 mg/kg/d administered orally on a once daily × 14 schedule. Significant tumor growth delay (TGD) and regressions were also observed in A375 tumors on this once-daily schedule. For example, five to eight complete or partial responses (CR/PR) and up to six tumor-free survivors (TFS) were observed (Table 1B). We also observed a schedule-dependent antitumor efficacy profile for RDEA119 in A375 tumor xenografts. For example, administering RDEA119 every other day at 100 mg/kg was less effective than daily dosing with either 25 or 50 mg/kg (Table 1B). Interestingly, when RDEA119 was dosed on a twice-daily schedule, it was more effective than once-daily schedules (Table 1B; Fig. 2*B*). This effect correlates with C_{min} levels as depicted in Fig. 2*B*. Taken together with the observation that A375 tumors rapidly regrew after the 14-day course of treatment (data not shown), our results suggest that continuous dosing with RDEA119 will be necessary to maximize *in vivo* antitumor activity.

RDEA119 also showed potent TGI in the human colon carcinoma Colo205 tumor xenograft. Doses of 25 and 50 mg/kg produced marked TGI during drug treatment (e.g., 25 mg/kg TGI = 123%; Table 1B, Colo205 study 1). Note that TGI >100% occurs when the tumor shrinks below its starting volume. Tumor regressions were also noted with seven PRs, two CRs, and two TFS observed within the nine animals treated with 25 mg/kg, and nine PRs seen in the 50 mg/kg treated group. An additional study was performed in Colo205-bearing animals to estimate an ED_{50} value using lower doses of RDEA119 on a once daily × 14 schedule (2.5–25 mg/kg, oral). In this experiment, we again found that RDEA119 produced marked TGI during drug treatment (e.g., 25 mg/kg TGI = 68%; Table 1B, Colo205 study 2). The ED_{50} value for TGI within this study ranged between 2.5 and 10 mg/kg for which 43% to 53% TGI was seen across these treatment arms (Table 1B).

In addition, we found that human A431 cells in which the ERK pathway is constitutively activated due to the overexpression of the EGF receptor (17) and human colon cancer HT-29 cells that harbor a *BRAF* V600E mutation also exhibited inhibition of tumor growth in the presence of RDEA119 (Table 1B). A dose of 25 mg/kg once daily × 14 produced 56% and 67% TGI for HT-29 and A431 tumors, respectively. During the 14 days of oral treatment with RDEA119, there was no significant loss in body weights across the 0 to 50 mg/kg treated animals (data not shown).

Pharmacokinetics of RDEA119 in mice. The pharmacokinetics of RDEA119 in mice was assessed over a 24-hour time course following oral exposure to a single dose of 25 mg/kg. RDEA119 was rapidly absorbed (T_{max} = 2 hours) with a total serum C_{max} of 9.85 μg/mL (see Fig. 3*A*). The C_{min} values at 12 and 24 hours were 1.37 and 0.03 μg/mL, respectively. The $t_{1/2}$ of RDEA119 following oral exposure in the mouse was 2.6 hours and the $AUC_{0\text{-}24h}$ was 55 (μg·h/mL). We simulated the pharmacokinetics of the more efficacious twice-daily 12.5 mg/kg oral dose of RDEA119 and project a total serum C_{max} of ~5 μg/mL (see Fig. 3*A*) with C_{min} values at 12 and 24 hours of 1.2 μg/mL. In comparison, the concentrations of RDEA119 necessary to inhibit (*a*) cellular pERK *in vitro* was 1.4 to 9.0 ng/mL (conversion from nmol/L to ng/mL = 0.572) or (*b*) anchorage-independent cell proliferation *in vitro* was 23 to 48 ng/mL across the cancer cell lines tested in 10% FBS (see Table 1A and B).

Pharmacokinetics/pharmcodynamics of RDEA119. The levels of pERK, a biomarker of MEK activity, were monitored over a 24-hour period in tumors, lung, and brain after a single dose of RDEA119 or another MEK inhibitor PD325901 at multiple dose levels. RDEA119 strongly suppressed pERK levels in Colo205 tumors for up to 12 hours compared with the vehicle-treated group (Fig. 3*B*). The relationship between MEK inhibition and plasma levels of RDEA119 is depicted in Fig. 4*B*. An EC_{50} value of 42 ng/mL (73 nmol/L) for MEK inhibition in tumors was obtained

Published OnlineFirst August 25, 2009; DOI: 10.1158/0008-5472.CAN-09-0679

Table 1. RDEA119 efficacy in cancer cell lines and tumor xenograft models

A. *In vitro* activity of RDEA119 in human tumor cells

Cell line	Tumor type	BRAF status	EC_{50} ± SD (nmol/L)		GI_{50} ± SD (nmol/L)*	
			1% FBS	+45 mg/mL hSA	Anchorage-dependent †	Anchorage-independent ‡
A375	Melanoma	V600E	8.7 ± 0.7	96 ± 18	67 ± 12	81 ± 17
SK-MEI-28	Melanoma	V600E	8.7 ± 1	77 ± 6	ND	ND
Colo205	Colon	V600E	2.5 ± 1.7	46 ± 5	89 ± 12	40 ± 8
HT-29	Colon	V600E	3.8 ± 1.7	120 ± 23	70 ± 12	ND
MDA-MB-231	Breast	G464V	ND	ND	>1,000	81 ± 56
A431	Epidermoid	Normal	5.1 ± 1.1	99 ± 27	>10,000	65 ± 19
BxPC3	Pancreas	Normal	15.8 ± 2.4	207 ± 29	ND	ND

B. Response summary of RDEA119 in xenograft models

Tumor model	Dose (mg/kg) and schedule	*n*§	% TGI‖	T-C¶	% TGD**	*P*††	Regression		
							PR‡‡	CR§§	TFS‖‖
A375 study 1	25, qd	10	72	25.3	143	<0.001	2	3	1
	50, qd	9	105	41.3	233	<0.001	1	7	6
	100, qod	10	63	16.1	91	<0.001	1	0	0
A375 study 2	25, qd	9	54	2.8	12	>0.05	0	0	0
	50, qd	9	68	4.7	21	<0.01	3	0	0
	12.5, bd	9	77	4.7	21	<0.05	7	0	0
	25, bd	9	108	37.1	163	<0.001	5	5	4
Colo205 study 1	25, qd	9	123	12.8	51	<0.05	7	2	2
	50, qd	9	125	18	71	<0.05	9	0	0
Colo205 study 2	2.5, qd	9	43	5.7	40	<0.001	0	0	0
	5, qd	10	50	4.8	33	<0.001	0	0	0
	10, qd	8	53	6.3	44	<0.001	0	0	0
	25, qd	10	68	9	63	<0.001	0	0	0
A431	25, qd	10	67	11.4	40	>0.05	0	0	0
	50, qd	9	84	16	56	<0.05	2	0	0
HT-29	25, qd	10	56	1.8	7	>0.05	0	0	0
	50, qd	9	90	6.6	27	>0.05	6	0	0

NOTE: Multiple xenograft models were tested with RDEA119, including A375 melanoma, Colo205 colon cancer, A431 epithelial human squamous carcinoma, and HT-29 colon adenocarcinoma.

Abbreviations: ND, not determined; qd, once daily; bd, twice daily; qod, every 2 days.

*GI_{50} = concentration resulting in 50% of the maximal growth inhibition induced by 1 μmol/L RDEA119.

† Anchorage-dependent growth was assessed after 48-h exposure to RDEA119.

‡ Anchorage-independent growth was assessed after 7-d exposure to RDEA119 in 0.15% agarose.

§*n* = number of animals at the end of 14-d dosing period.

‖% TGI = 100 * [1 − (RDEA119-treated tumor $volume_{final}$ − tumor $volume_{initial}$) / (vehicle-treated tumor $volume_{final}$ − tumor $volume_{initial}$)]. Tumor volumes on day 15 for all treated groups differed from vehicle-treated tumor volumes ($P < 0.01$, as determined by ANOVA).

¶T-C = difference between median time to end point in days between treated (T) and control (C) groups.

**Calculated using the formula [100 * (T − C) / C], where T = median time to end point for treatment group and C = median time to end point for vehicle control group.

†† *P* value = log-rank test was used to analyze the statistical significance of the differences between time to end point for treated and control groups.

‡‡ Tumor size is ≤30% of tumor size on day 1 but ≥13.5 mm^3 for one or more measurements in the study.

§§No measurable tumor mass (<13.5 mm^3) for three consecutive measurements during the course of the study.

‖‖No measurable tumor mass (<13.5 mm^3) at the end of the study.

in this study. In brain samples, MEK activity was not sufficiently inhibited by RDEA119 to calculate an EC_{50} value but would likely require >3,000 ng/mL in plasma to achieve 50% inhibition of MEK activity in brain (Fig. 3*C*). Interestingly, other MEK inhibitors block pERK equally well in brain and in lung. Figure 4*A* to *D* shows a comparison of pERK inhibition by RDEA119 and PD325901 at 10 mg/kg in the three different tissues in nude mice. In all three tissues, the PD325901 compound blocks phosphorylation of ERK

Published OnlineFirst August 25, 2009; DOI: 10.1158/0008-5472.CAN-09-0679

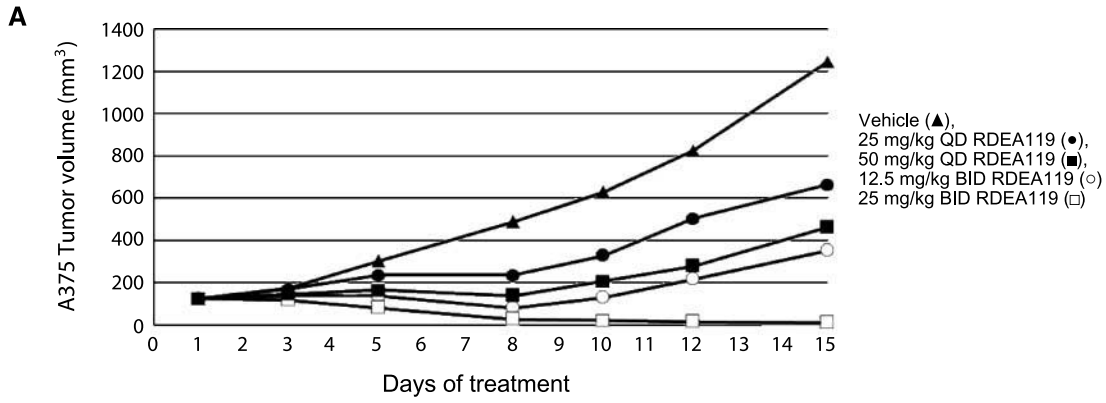

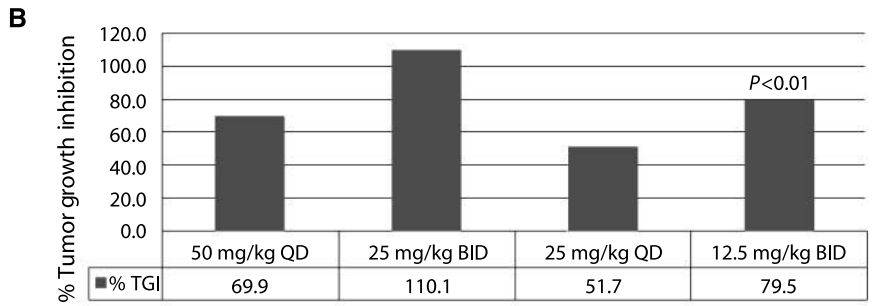

AUC (μg·h/mL)	132.5	117	66.5	78
*C*max (μg/mL)	23.8	10.2	11.9	7.8
*C*min (μg/mL)	0.06	1.24	0.03	0.49
*C*min free Fraction (ng/mL)	0.117	2.48	0.059	0.986

Figure 2. Efficacy of RDEA119 on the growth of human melanoma A375 tumors in *nu/nu* mice. Female *nu/nu* mice were implanted with A375 tumor cells, which were allowed to grow to 80 to 185 mm^3, and then treated for 14 d with RDEA119 administered orally once or twice a day. *A,* average tumor volumes are graphed for the vehicle- and RDEA119-treated groups. Average tumor volumes of mice dosed orally with vehicle (▲), 25 mg/kg RDEA119 once daily (●), 50 mg/kg RDEA119 once daily (■), 12.5 mg/kg RDEA119 twice daily (○), or 25 mg/kg RDEA119 twice daily (□) are shown for the indicated day. *B,* animals were treated from days 1 to 14. C_{max}, maximum or "peak" concentration of a drug observed after its administration; C_{min}, minimum or "trough" concentration of a drug observed after its administration and just before the administration of a subsequent dose; *AUC,* area under the curve for a given dose otherwise known as the overall exposure.

similarly. In contrast, RDEA119 exhibits tissue selectivity, showing little or no inhibition in brain, significantly lower effect in lung, and sustained efficacy in tumor tissue. The levels of RDEA119 in the lung are similar to the concentration in plasma, whereas the levels in the brain are much lower than in the plasma, suggesting that RDEA119 has low central nervous system (CNS) penetration. In contrast, concentrations of PD325901 are higher in the brain than in plasma (Fig. 4*A–D*).

Rat tissue samples were evaluated for pERK inhibition 48 hours after oral dosing with RDEA119 and PD325901. MEK activity in the brain was inhibited by PD325901 in a dose-dependent manner. No significant inhibition of MEK was shown for RDEA119 at any dose tested. Plasma concentrations were correlated with MEK inhibition in brain homogenates. Figure 4 shows dose-dependent inhibition of brain pERK levels only for PD325901, which had an EC_{50} value of 641 ng/mL. There was very little pERK inhibition in the brain for RDEA119 (Fig. 4*A–B*).

We next compared the efficacy of the PD and RDEA compounds in two different xenograft models (Table 2). These were a colon cancer line, Colo205, and a melanoma line, A375. These were tested in a standard xenograft model with oral dosing for both compounds for 14 days. Tumor volumes were measured along with tumor-free survival. The data are shown in tabular form for both experiments. In both colon and melanoma models, the efficacy and potency for each compound were similar and not significantly different. Both compounds significantly suppressed tumor volume in treated mice. The MEK inhibitors showed a higher number of tumor-free survivors in both models compared with the reference treatment.

Discussion

The attractiveness of MEK as a pharmaceutical target has been enhanced by the discovery of highly selective non–ATP-competitive inhibitors of MEK1/2 (18–21). Such selectivity is achieved by the interaction of the inhibitor with a hydrophobic pocket in MEK that interferes with subsequent binding and hydrolysis of ATP (10). Through cocrystallization of RDEA119 with human MEK1, we have found that RDEA119 binds in this MEK hydrophobic pocket and blocks MEK enzymatic activity (Fig. 1).

First-generation MEK inhibitors (e.g., CI-1040) had poor exposure in patients, preventing sustained MEK inhibition in tumor tissue

Published OnlineFirst August 25, 2009; DOI: 10.1158/0008-5472.CAN-09-0679

(22–24). Second-generation inhibitors (e.g., PD325901), although significantly more potent and more water soluble, have been hampered by side effect issues, including ocular and neurologic toxicities, presumably due to accumulation of such agents in the brain and other neural tissue (25). Thus, significant interest has arisen in the field for the discovery and development of potent and selective MEK inhibitors that lack CNS retention. As such, we focused our efforts on designing a MEK inhibitor that retains high potency and selectivity to MEK over other kinases and good pharmaceutical properties (solubility, oral bioavailability, etc.) while avoiding CNS retention compared with first-generation agents such as PD325901.

The data described in this article show that RDEA119 is a highly potent and selective inhibitor of MEK1/2 activity through its interaction with MEK. X-ray crystallographic analysis reveals that RDEA119 binds to an allosteric pocket adjacent to the ATP binding site, locking the enzyme in a catalytically inactive conformation. When bound to MEK, RDEA119 interacts directly with ATP, the activation loop, and other surrounding protein residues through both hydrogen bonding and hydrophobic interactions, resulting in significant affinity for the binding pocket. RDEA119 had preferential growth-inhibitory activity in cancer cells harboring the *BRAF* gain-of-function mutation, V600E, consistent with the activities of other MEK inhibitors

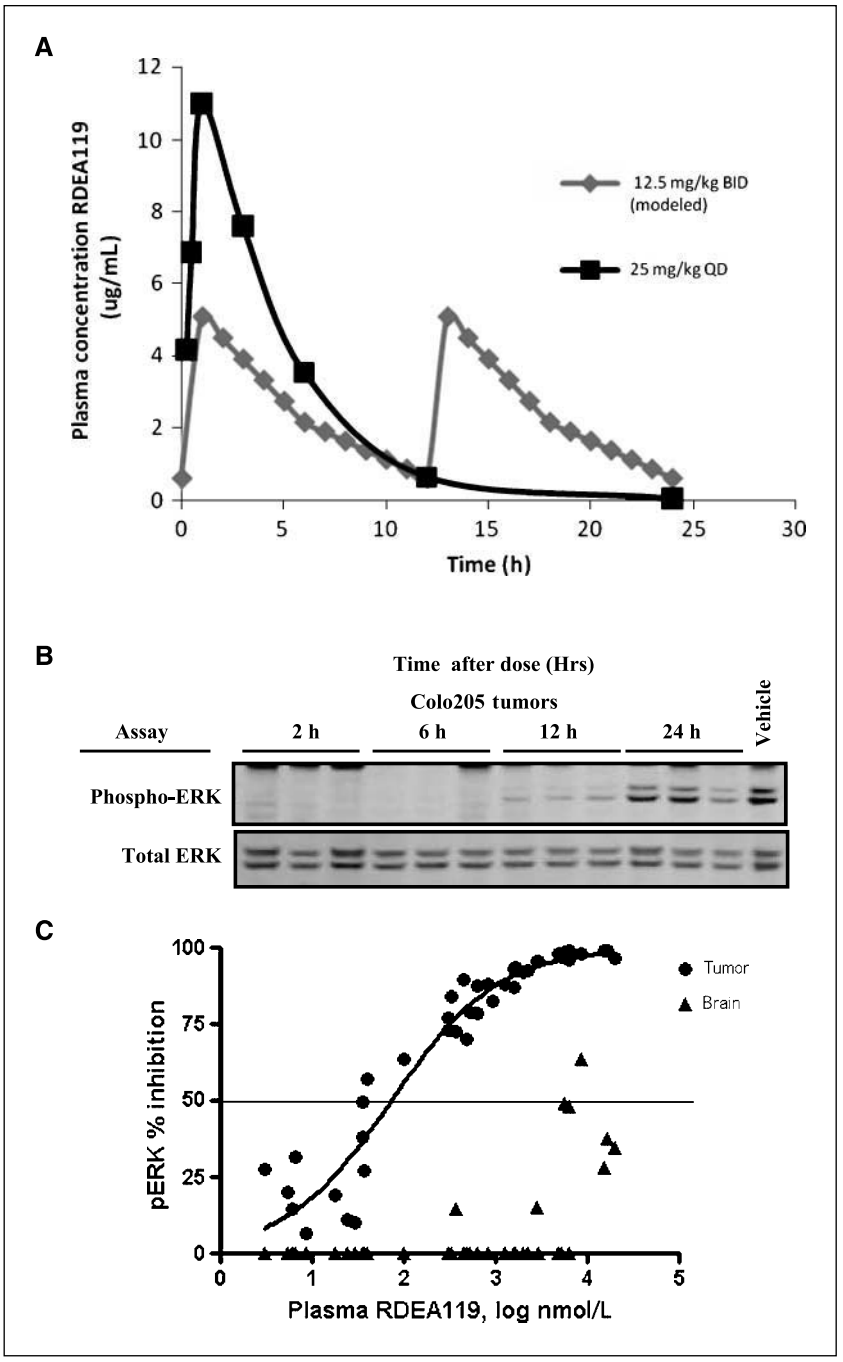

Figure 3. *A,* mouse plasma concentrations of RDEA119 in response to a 25 mg/kg dose and predicted response to 12.5 mg/kg twice daily dose. ■, plasma concentrations in μg/mL are plotted for 25 mg/kg dose of RDEA119. The C_{max} is 15.4 and the $t_{1/2}$ is 1.85. ♦, predicted values for 12.5 mg/kg based on a noncompartmental model. *B,* pharmacokinetic/pharmacodynamic study of RDEA119. Western blot of pERK and total ERK from tumors collected from mice at the indicated time points in the 25 mg/kg dose group. *C,* inhibition of pERK in tumors and brain from individual animals from all the dose groups and time points are graphed with their corresponding plasma concentration of RDEA119.

Published OnlineFirst August 25, 2009; DOI: 10.1158/0008-5472.CAN-09-0679

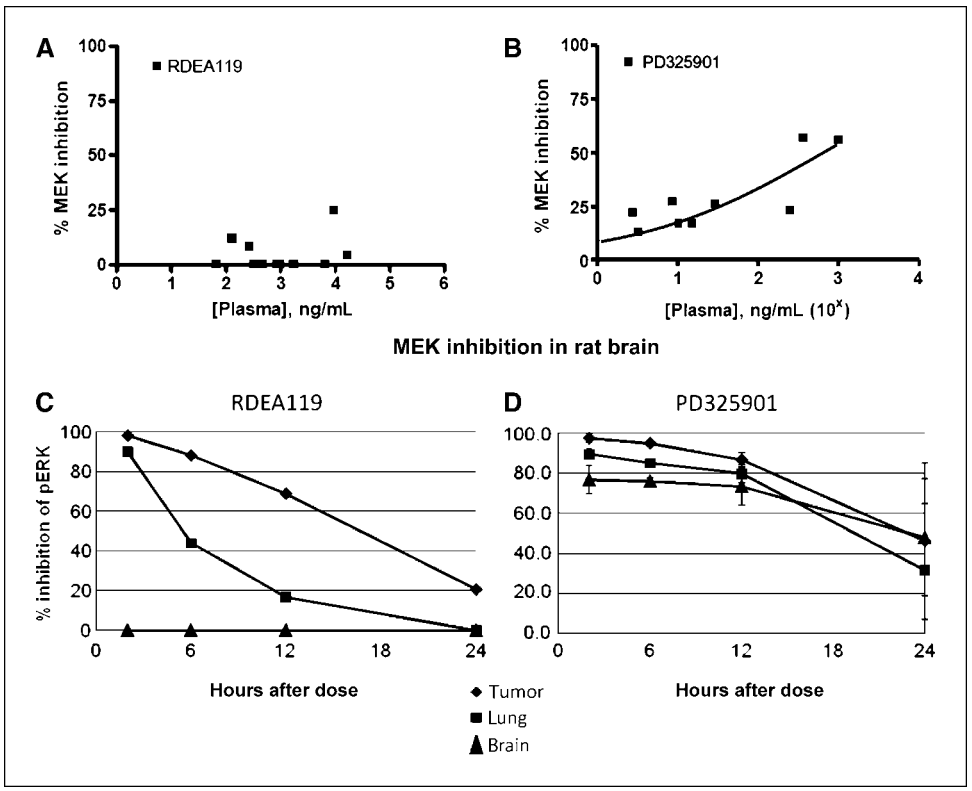

Figure 4. *A* and *B*, plasma levels of MEK inhibitor and MEK inhibition in rat brain. Plasma MEK inhibitor levels of RDEA119 (*A*) and PD325901 (*B*) are plotted against % MEK inhibition in brain. One hundred percent pERK levels (0% MEK inhibition) were determined in vehicle-treated rats. *C* and *D*, inhibition of pERK activity in brain, lung, and Colo205 tumor in nude xenograft mice treated with 10 mg/kg RDEA119 (*C*) or 10 mg/kg PD325901 (*D*).

(13, 18, 26). However, this differential sensitivity was only seen in our hands under anchorage-dependent (cell growth on plastic) conditions. Anchorage-independent growth in a semisolid medium showed no clear sensitivity differences in the cancer cell lines tested. Further studies will be necessary to explain the mechanistic basis for this differential sensitivity. However, it seems that growth on plates reduces or bypasses the need for MEK activity for cell proliferation in some cell lines.

The antitumor activity of RDEA119 was shown across a variety of human tumor xenografts, including the human melanoma A375 tumor and the human colon cancer xenograft Colo205. Both tumors express activated *BRAF* mutations (see Table 1A). We also

Table 2. RDEA119 and PD325901 efficacy in Colo205 and A375 tumor xenograft models

Group	*n*	Colo205 xenograft		Median TTE	T-C	% TGD	No. PR	No. CR	No. TFS
		Agent	mg/kg						
1	9	Vehicle	—	41.0			0	0	0
2	9	Paclitaxel	30	74.0	33.0	80%	5	0	0
3	9	PD325901	25	42.3	1.3	3%	2	0	0
4	9	PD325901	50	60.0	19.0	46%	1	2	2
5	9	RDEA119	25	47.9	6.9	17%	1	2	2
6	9	RDEA119	50	59.1	18.1	44%	4	0	0
Group	*n*	A375 xenograft		Median TTE	T-C	% TGD	No. PR	No. CR	No. TFS
		Agent	mg/kg						
1	9	Vehicle	—	16.0			0	0	0
2	10	Paclitaxel	30	17.4	1.4	9%	0	0	0
3	10	PD325901	25	25.0	9	56%	1	1	1
4	21	PD325901	50	60.0	44.0	275%	3	12	12
5	10	RDEA119	25	17.9	1.9	12%	0	1	1
6	21	RDEA119	50	60.0	44.0	275%	1	18	15

Abbreviation: TTE, time to end point.

Published OnlineFirst August 25, 2009; DOI: 10.1158/0008-5472.CAN-09-0679

observed dosing schedule dependency in the degree of antitumor activity observed *in vivo* (see Table 1B and Fig. 2), with twice-daily dosing being more effective than less frequent dosing. Pharmacokinetic analysis of RDEA119 concentrations in the plasma of mice was assessed from a single dose of RDEA119 (see Fig. 3*A*). The twice-daily and every other day pharmacokinetics of RDEA119 were then modeled from this actual data set. Superimposition of these pharmacokinetic profiles illustrated that the degree of antitumor activity seen with RDEA119 in these human tumor xenografts is more likely to correlate with maintaining plasma levels of RDEA119 above 1,240 ng/mL (from C_{min} at 25 mg/kg twice daily A375 xenograft) for 24 hours rather than high peak levels (C_{max}). This is consistent with findings that once RDEA119 dosing stopped, tumors rapidly regrew in mice harboring residual tumor mass. These data suggest that continuously inhibiting MEK activity in a patient's tumor throughout the period between doses will be important to achieve and sustain antitumor efficacy.

To assess the potential for brain penetration and activity, we compared the ability of RDEA119 to inhibit pERK levels in the brain, lung, and tumor tissues of tumor-bearing mice and found at least that 76-fold lower plasma levels of RDEA119 were required to inhibit 50% of the pERK level in tumor versus brain. Testing of other MEK inhibitors, including PD325901, revealed little or no difference in brain, tumor, and lung penetration versus plasma for these other compounds (Figs. 3*B* and *C* and 4*A–D*). We have tested mouse MEK *in vitro* and *in vivo* and see no difference in affinity or inhibitory activity between the species (data not shown). These experiments suggest that RDEA119 exhibits reduced potential for brain-related side effects and may preferentially accumulate in tumor tissue. To ensure that comparable pERK suppression in tumors correlated with efficacy *in vivo*, we tested both compounds side by side in two 14-day xenograft models. As shown in Table 2, each compound was equally efficacious at blockade of tumor growth at both 25 and 50 mg/kg. These data are consistent with the pERK suppression detected in tumors from the 1-day dose experiment for both compounds (Fig. 4) and is also consistent with the comparable affinities for the MEK enzyme for these two compounds. The differences noted for these molecules give further weight to the notion that alterations in chemical structure with similar effects on affinity can differentially affect activity *in vivo*.

In summary, RDEA119 is a highly potent and selective inhibitor of MEK1/2 whose encouraging preclinical pharmacology profile supported entry into development for the treatment of cancer. RDEA119 is currently undergoing phase I clinical trials in late-stage cancer patients refractory or intolerant to other anticancer therapies.

Disclosure of Potential Conflicts of Interest

All authors were employees of sponsoring company.

Acknowledgments

Received 2/25/09; revised 4/23/09; accepted 6/3/09; published OnlineFirst 8/25/09.

The costs of publication of this article were defrayed in part by the payment of page charges. This article must therefore be hereby marked *advertisement* in accordance with 18 U.S.C. Section 1734 solely to indicate this fact.

We thank Shunqi Yan for provision of information about the X-ray structural work, Kay Meshaw of Piedmont labs and Heli Walker for technical assistance, and Anneke Raney for reviewing the manuscript.

References

1. Hayat MJ, Howlader N, Reichman ME, Edwards BK. Cancer statistics, trends, and multiple primary cancer analyses from the Surveillance, Epidemiology, and End Results (SEER) Program. Oncologist 2007;12:20–37.
2. Slattery ML, Murtaugh MA, Quesenberry C, Caan BJ, Edwards S, Sweeney C. Changing population characteristics, effect-measure modification, and cancer risk factor identification. Epidemiol Perspect Innov 2007;4:10.
3. Pang RW, Poon RT. From molecular biology to targeted therapies for hepatocellular carcinoma: the future is now. Oncology 2007;72 Suppl 1:30–44.
4. Raben D, Helfrich B, Bunn PA, Jr. Targeted therapies for non-small-cell lung cancer: biology, rationale, and preclinical results from a radiation oncology perspective. Int J Radiat Oncol Biol Phys 2004;59:27–38.
5. Friday BB, Adjei AA. Advances in targeting the Ras/Raf/MEK/Erk mitogen-activated protein kinase cascade with MEK inhibitors for cancer therapy. Clin Cancer Res 2008;14:342–6.
6. Wang D, Boerner SA, Winkler JD, LoRusso PM. Clinical experience of MEK inhibitors in cancer therapy. Biochim Biophys Acta 2007;1773:1248–55.
7. Katz M, Amit I, Yarden Y. Regulation of MAPKs by growth factors and receptor tyrosine kinases. Biochim Biophys Acta 2007;1773:1161–76.
8. Solit DB, Garraway LA, Pratilas CA, et al. BRAF mutation predicts sensitivity to MEK inhibition. Nature 2006;439:358–62.
9. Leboeuf R, Baumgartner JE, Benezra M, et al. BRAFV600E mutation is associated with preferential sensitivity to mitogen-activated protein kinase kinase inhibition in thyroid cancer cell lines. J Clin Endocrinol Metab 2008;93:2194–201.
10. Ohren JF, Chen H, Pavlovsky A, et al. Structures of human MAP kinase kinase 1 (MEK1) and MEK2 describe novel noncompetitive kinase inhibition. Nat Struct Mol Biol 2004;11:1192–7.
11. Shaul YD, Seger R. The MEK/ERK cascade: from signaling specificity to diverse functions. Biochim Biophys Acta 2007;1773:1213–26.
12. Estep AL, Palmer C, McCormick F, Rauen KA. Mutation analysis of BRAF, MEK1 and MEK2 in 15 ovarian cancer cell lines: implications for therapy. PLoS ONE 2007;2:e1279.
13. Wang JY, Wilcoxen KM, Nomoto K, Wu S. Recent advances of MEK inhibitors and their clinical progress. Curr Top Med Chem 2007;7:1364–78.
14. Otwinoski Z, Minor W. Processing of X-ray diffraction data collected in oscillation mode. Methods Enzymol 1997;276:307–26.
15. Brunger AT, Adams PD, Clore GM, et al. Crystallography & NMR system: a new software suite for macromolecular structure determination. Acta Crystallogr D Biol Crystallogr 1998;54:905–21.
16. Bos JL. ras oncogenes in human cancer: a review. Cancer Res 1989;49:4682–9.
17. Thompson DM, Gill GN. The EGF receptor: structure, regulation and potential role in malignancy. Cancer Surv 1985;4:767–88.
18. Yeh TC, Marsh V, Bernat BA, et al. Biological characterization of ARRY-142886 (AZD6244), a potent, highly selective mitogen-activated protein kinase kinase 1/2 inhibitor. Clin Cancer Res 2007;13:1576–83.
19. Han S, Zhou V, Pan S, et al. Identification of coumarin derivatives as a novel class of allosteric MEK1 inhibitors. Bioorg Med Chem Lett 2005;15:5467–73.
20. Wallace EM, Lyssikatos JP, Yeh T, Winkler JD, Koch K. Progress towards therapeutic small molecule MEK inhibitors for use in cancer therapy. Curr Top Med Chem 2005;5:215–29.
21. Mallon R, Feldberg L, Kim S, et al. Identification of 4-anilino-3-quinolinecarbonitrile inhibitors of mitogen-activated protein/extracellular signal-regulated kinase 1 kinase. Mol Cancer Ther 2004;3:755–62.
22. Lorusso PM, Adjei AA, Varterasian M, et al. Phase I and pharmacodynamic study of the oral MEK inhibitor CI-1040 in patients with advanced malignancies. J Clin Oncol 2005;23:5281–93.
23. Rinehart J, Adjei AA, Lorusso PM, et al. Multicenter phase II study of the oral MEK inhibitor, CI-1040, in patients with advanced non-small-cell lung, breast, colon, and pancreatic cancer. J Clin Oncol 2004;22:4456–62.
24. Allen LF, Sebolt-Leopold J, Meyer MB. CI-1040 (PD184352), a targeted signal transduction inhibitor of MEK (MAPKK). Semin Oncol 2003;30:105–16.
25. Brown AP, Carlson TC, Loi CM, Graziano MJ. Pharmacodynamic and toxicokinetic evaluation of the novel MEK inhibitor, PD0325901, in the rat following oral and intravenous administration. Cancer Chemother Pharmacol 2007;59:671–9.
26. Davies BR, Logie A, McKay JS, et al. AZD6244 (ARRY-142886), a potent inhibitor of mitogen-activated protein kinase/extracellular signal-regulated kinase kinase 1/2 kinases: mechanism of action *in vivo*, pharmacokinetic/pharmacodynamic relationship, and potential for combination in preclinical models. Mol Cancer Ther 2007;6:2209–19.

Cancer Research
The Journal of Cancer Research (1916–1930) | The American Journal of Cancer (1931–1940)

AACR American Association for Cancer Research

RDEA119/BAY 869766: A Potent, Selective, Allosteric Inhibitor of MEK1/2 for the Treatment of Cancer

Cory Iverson, Gary Larson, Chon Lai, et al.

Cancer Res 2009;69:6839-6847. Published OnlineFirst August 25, 2009.